Regenerated and Graft Copolymer Fibers from Steam-Exploded Wheat Straw: Characterization and Properties

B. FOCHER,[1] A. MARZETTI,[1] E. MARSANO,[2] G. CONIO,[3] A. TEALDI,[3] A. COSANI,[4] M. TERBOJEVICH[4]

[1] Stazione Sperimentale per la Cellulosa, Carta e Fibre Tessili Vegetali ed Artificiali, P.zza L. da Vinci 26-20133 Milano, Italy

[2] Dipartimento di Chimica e Chimica Industriale, Università di Genova, Via Dodecaneso 31-16146 Genova, Italy

[3] IMAG, CNR, Via De Marini 6-16149 Genova, Italy

[4] Centro Studi sui Biopolimeri, CNR, Via Marzolo 1-35131 Padova, Italy

Received 25 February 1997; accepted 10 June 1997

ABSTRACT: Steam explosion treatment has been proven to effectively induce such marked modifications to the chemical and supramolecular structure of wheat straw cellulose as to make this cellulose a suitable raw for dissolving processes. Regenerated and poly(acrylonitrile) (PAN) and poly(methyl methacrylate) (PMMA) grafted wheat straw fibers obtained on the laboratory scale were characterized by various techniques (X-ray diffraction, cross polarization-magic angle spinning (CP-MAS) ^{13}C nuclear magnetic resonance and vibrational spectroscopy, scanning electron microscopy, differential scanning calorimetry), and the relationships between the morphological–structural features and physicomechanical and end-use properties have been evidenced. © 1998 John Wiley & Sons, Inc. J Appl Polym Sci **67:** 961–974, 1998

Key words: regenerated fibers; graft copolymers; wheat straw; steam explosion

INTRODUCTION

In recent years, there has been an increasing demand for new materials with tailored technological properties like low density, high modulus, high strength, and toughness, combined with friendly environmental impact. This demand has led to renewed interest in the lignocellulosic biomass of perennial and annual plants as the raw material for the production of a variety of conventional and advanced polymeric materials.

Wheat straw is probably one of the most promising, readily available, nonwoody raw materials; however, its multicomponent nature and poor compatibility with synthetic matrices are severe drawbacks to its industrial exploitation. Thus, in an effort to improve the utilization of wheat straw, investigations have been made into alternative innovative processes able to cope with these draw backs.

The steam explosion (STEX) process was introduced to defibrate wood and fractionate lignocellulosics into individual components.[1–4] The process brings about a marked increase in extractable lignin and an increasing reactivity of cellulose towards chemical and biochemical agents.[4] The advantages of the STEX process lie in its very short treatment times; the absence of, or reduced need, for chemicals; and its low energy requirements, also in the later transformation steps. Furthermore, STEX, through adjustments to the working conditions, has the potential to be used for the integrated production of various

Correspondence to: B. Focher.

Journal of Applied Polymer Science, Vol. 67, 961–974 (1998)
 CCC 0021-8995/98/060961-14

cellulosic products (papermaking fibers, dissolving pulps, reinforcement fibers, and fermentation substrates).[4]

In the present work, the effect of STEX treatment on the structural features and reactivity of wheat straw has been studied, and an investigation has been made into the utilization of steam exploded straw for the production of regenerated lignocellulosic and their graft copolymer fibers.

EXPERIMENTAL

Materials and Methods

The STEX laboratory trials were carried out on a DELTALAB EC 300 laboratory scale pilot. Wheat straw and its internode-enriched fraction were steam-exploded at 225°C for 3 min in the pilot plant of the Centre Technique de la Papeterie (Grenoble, France) and used for the preparation of regenerated fibers.

A bleaching treatment was carried out after extracting the STEX fibers with 2% (w/w) soda solution at 80°C for 2 h (batch ratio: 3 g solution/g material), using $NaBH_4$ to quench peeling reactions. After washing with water, the material was bleached with a buffered (pH 4.8) solution of 0.3% sodium chlorite (batch ratio: 40 g solution/g material) at 70°C for 2 h. The bleached pulps were then washed with water and air-dried. The composition of the untreated wheat straw samples was in accordance with the literature.[5] The lignin content of the STEX samples was determined according to standard methods (TAPPI T222 om 83 and UM 250). Reducing sugars were determined by ferricyanide method.[6]

In order to obtain regenerated fibers, the unbleached and bleached STEX products were dissolved in dimethylacetamide (DMAc)–LiCl 7%; before the spinning, the more concentrated solutions were centrifuged to remove any residues. Grafting reactions were carried out in the heterogeneous phase at 55°C for 1–2 h under nitrogen stream on STEX internode and STEX–NaOH extracted internode fibers, in $10^{-3}M$ H_2SO_4 using Fe^{2+}/H_2O_2 as the initiator system and adding acrylonitrile (AN) and methylmetacrylate (MMA) as monomers. After reaction, the products were separated by filtration, washed with water, and dried under vacuum. Poly(acrylonitrile)(PAN) and poly(methyl methacrylate) (PMMA) homopolymers were removed in Soxhlet with dimethylformamide (DMF) and acetone, respectively.

Weighed amounts of bleached STEX pulps of graft copolymers were dissolved in DMAc at 150°C (activation step), the heating being stopped after 30 min. When the temperature of the mixture had dropped to 120°C, dry LiCl was added (7%), and the mixture left under stirring at room temperature overnight until complete dissolution.

The carbanilation reaction[7] of the bleached STEX straw (0.2 g) was carried out in DMAc-5% LiCl solution (20 mL) under different temperature (60–80°C) and time (2–3 h) conditions, adding phenylisocyanate (2 mL) in the presence or absence of a catalytic amount of pyridine (0.4 mL). After cooling, methanol was added to eliminate any excess of phenylisocyanate, and the mixture precipitated with MeOH–H_2O (70 : 30), washed with water, and dried under vacuum. The degree of substitution was determined by elemental analysis.

Viscosity was determined using a multigradient suspended-level Ubbelohde viscometer at 25.0 ± 0.1°C and ranged between 1.1 and 1.6. Dilution was carried out directly in the viscometer, and intrinsic viscosity $[\eta]$ values were calculated by the Huggins equation.[8]

Light scattering (ls) measurements were performed at 20°C using a Sofica Model 4200 photometer with cylindrical cells immersed in toluene. Nonpolarized laser light (633 nm) was used; scattering angles (θ) ranged between 30 and 150°. A Rayleigh ratio $R_{90°} = 8.96 \times 10^{-6}$ cm^{-1} was used for calibration of the instrument with benzene.[9] Solutions and solvents were clarified by centrifugation at 25,000g for 3 h. The data were treated as previously reported.[10]

Gel permeation chromatography (GPC) measurements were carried out using a Knauer 6400 pump, a Rheodyne injector, and a differential refractometer (Erma CR, ERC-7512). Phenogel columns (7.8 × 30 mm) packed with crosslinked polystyrene (PHOOH 0445KO, 0446KO, 0447KO) were eluted with stabilized tetrahydrofuran (THF), at a flow rate of 1 mL min at room temperature. Polymer concentration was 0.1%, and the injected volume 100 μL. Two different spinning lines were used.

1. A wet spinning line, with a 100 μm spinnerette die with a length-to-diameter ratio of 1. The extrusion speed V_0 was fixed at 7.9 m min, corresponding to a shear rate at the spinnerette of 10,500 s^{-1}. The monofilament, extruded in H_2O at 20°C and collected after the coagulation bath by a set

of spools (V_1 take-up speed), passed into a water bath, and then through a second set of spools (V_2 take-up speed); the filament was finally wound up by a spoon, operated at V_r take-up speed.[11] The V_2/V_1 and V_r/V_1 ratios were invariably kept equal to 1. Different V_1/V_f ratios were used, with V_f being the speed of the freely extruded filament. The spools were washed in running water for 2 h, dried under vacuum at 40°C for 24 h, and stored under $CaCl_2$.

2. A dry jet spinning line was used, using a spinnerette with capillary diameter of 300 μm, and a length-to-diameter ratio of 4, V_0 = 28 and 42 m/min, corresponding, respectively, to shear rates of 12,500 and 18,700 s^{-1}. The coagulation bath was approximately 3 m long, and the air gap between the spinnerette and the water surface of the coagulation bath was 2.5 cm. The fibers were wound onto spools at various V_1 take-up speeds, the wound spools were then washed in water for 24 h to ensure complete removal of the solvent, air-dried for 8 h, and vacuum oven-dried for 24 h at 40°C.

No post-spinning treatment for fibers obtained from both spinning lines was performed, and different V_1/V_0 ratios (DR) were used.

Fiber characterization was performed using a scanning electron microscopy (SEM) electron microscope (Philips 515), observing the morphological features of the lateral surface of the intact fiber first, then breaking the fiber and observing the fractured surface.

The mechanical properties of single regenerated and graft copolymer fibers were measured (ASTM 3822 method) using an Instron 1120 instrument with a 50 mm gauge length at a strain rate of 10 mm min. The elastic modulus (E), breaking strength (σ_b) and elongation to break (ε_b) were calculated as the average of ten measurements from load–elongation curves. The initial modulus and breaking strength are expressed in GPa, assuming that 1 GPa = 7.3 g den (value for pure cellulose).

The Raman spectra were obtained with a Bruker FRA 106 accessory for the IFS66 Fourier transform infrared (FTIR) spectrometer, using laser excitation at 1064 nm (Nd : YAG laser, 0.2 W). The 90° to the incident beam scattering arrangement was used, and no correction was made for spectral response. One hundred scans of 8 cm^{-1} resolution were averaged to achieve an adequate signal-to-noise ratio.

To collect the polarized spectra, the Raman radiation was passed through a Glan Thompos crystal polarizer, and the polarization changed by turning a half-wave plate in the polarization accessory. The polarized Raman radiation was then focused on the sample of the fiber, and the scattered light passed through an analyzer. Rotating the half-wave plate with respect to two orthogonal positions of the analyser provided four independent polarized measurements for the given sample geometry. The differences between the spectra recorded with the polarization scrambler inserted are, according to the supplier, negligible, indicating that no further correction is required to improve the result.[12]

The CP-MAS ^{13}C nuclear magnetic resonance (NMR) spectra were obtained with a Bruker CXP-300 (75 MHz) spectrometer, using cross polarization time 1 msec, repetition time, and the ^1H 90 pulse 10 s and 3.5 μs, respectively; width at half-height of glycine was 27 MHz; chemical shift was measured with respect to TSP; 3000–5000 scans at the rotation speed of 3.4 KHz were collected.

Wide-angle X-ray measurements of the regenerated fibers were obtained at 20°C using a Siemens D-500 instrument, the operating voltage and current being 40 kV and 18 mA, respectively. The selected orientation measurements of the crystallites were collected at $2\theta = 20°$ by a transmission specimen carrier (0.008 rpm), while the crystallinity index (Cr.I) was determined according to the method of Segal et al.[13]

For microscopy measurements, the dichroic index (I_{dr}) was assessed using a Leitz microscope equipped with a monochromatic light source operating at 550 nm, and the intensity of the transmitted light was measured by a galvanometer. The fibers, dyed with an aqueous solution of red Congo (0.1% w/v) for 15 h at 20°C, were mounted on slides with cedar oil. $I_\parallel$ and $I_\perp$ intensities of transmitted light, in orthogonal directions with respect to the fiber axis, were measured. The dichroic index was calculated according to the following formula:[14]

$$I_{dr} = \frac{K_\parallel - K_\perp}{K_\parallel} \cdot 100$$

Differential scanning calorimetry (DSC) analysis of the grafted fibers was performed with a Perkin–Elmer DSC-4, heating the samples (10 mg) from 20 to 200°C at a scan rate of 20°C min.

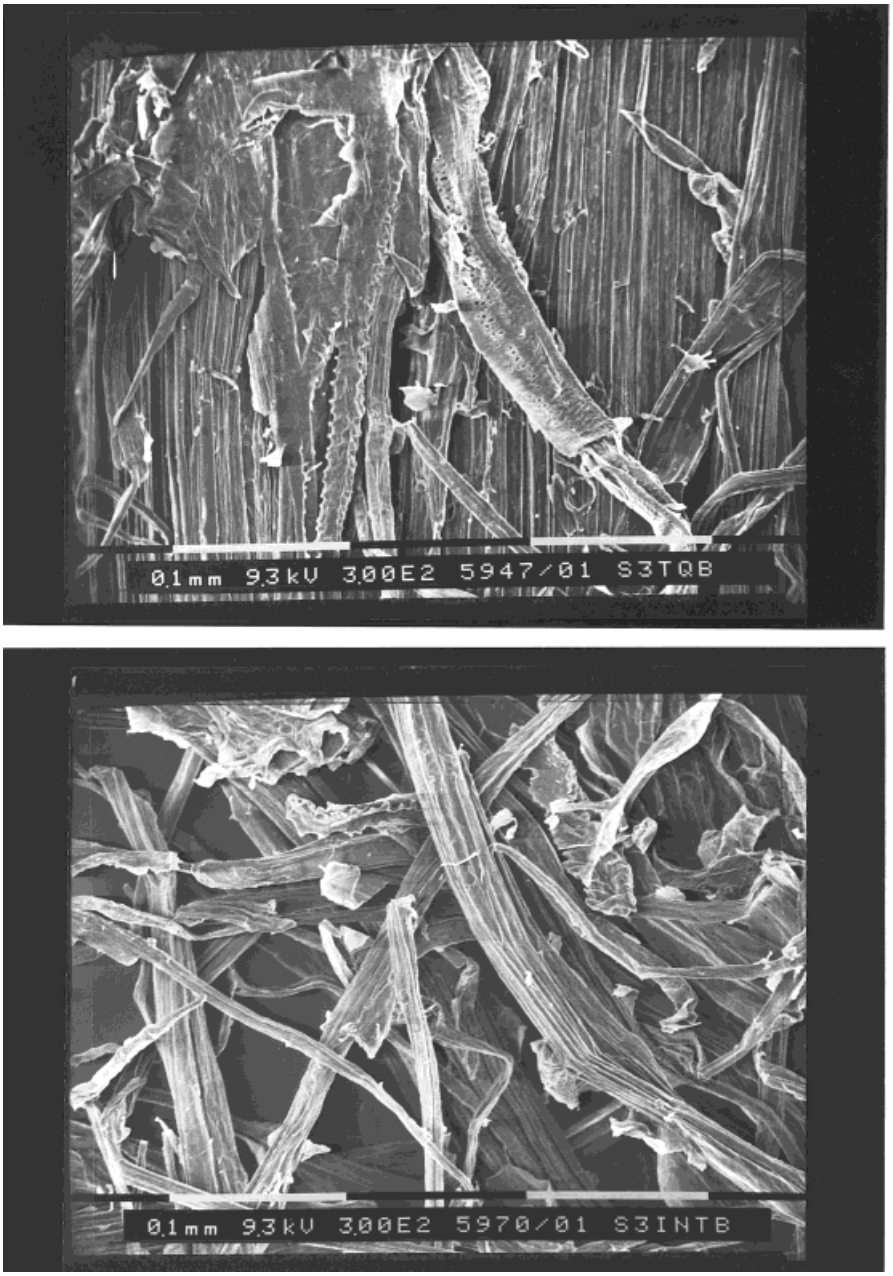

Figure 1 SEM microphotographs of (a) whole straw, (b) internode fraction, and (c) STEX internodes at 300×.

RESULTS AND DISCUSSION

Steam Explosion and Fractionation of Wheat Straw

The primary target of this work was to verify the suitability of STEX as a pretreatment in obtaining dissolving pulps and reinforcement fibers from straw. Included in this verification was an evaluation of how, and to what degree, the working conditions of STEX influence the characteristics, solubility in solvent systems (such as DMAc/LiCl), and the spinning properties of STEX pulps.

Laboratory experiments were carried out on whole straw that had been steam-exploded at different temperatures (210–230°C) and for different residence times (1–6 min). It was found that by regulating the STEX working conditions, pulps having different characteristics could be obtained, with the composition and degree of polymerization of the cellulose component of these pulps be-

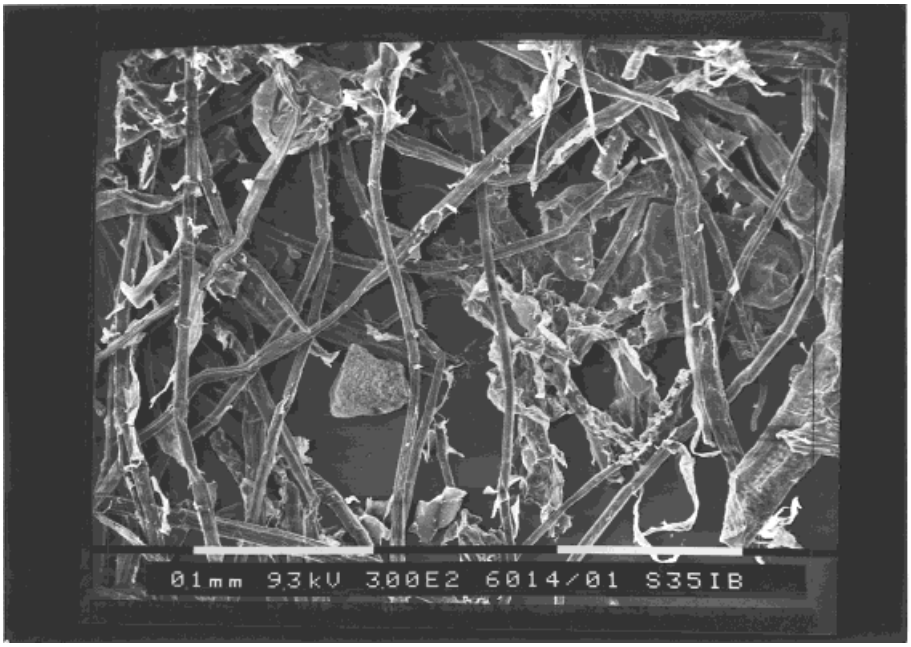

c)

Figure 1 (*Continued from the previous page*)

ing greatly dependent on the severity of the STEX treatment. In fact, in all the tests, it was found that increasing the temperature without significantly altering the residence time led to a drastic reduction in hemicellulose content and the degree of polymerization (DP_v) of cellulose; whereas lignin underwent chemical modification and partial depolymerization. Furthermore, it was observed that the degree of straw fiber aggregation, seen with the optical and electron microscope, is markedly modified as a function of the STEX conditions; at the highest temperatures, the fibers were almost completely dispersed.

Following these indications, both the wheat straw and its internode-enriched fraction were steam-exploded at 225°C for 3 min. The STEX fibers from both were assessed from the point of view of using them as starting material to produce regenerated fibers, with every effort being made to identify any differences that could be relevant to obtaining end products with different properties.

The characterization, by SEM, of the whole straw and the internode fraction revealed a more open material in the internode fraction [Fig. 1(a) and (b)], but no differences were observed in the surface features of the fibers, with both samples being quite smooth [Fig. 2(a)]. The main action of the steam explosion was to separate out single fibers from the bundles [Fig. 1(c)] and increase the fiber surface area, this latter phenomenon being evidenced at the morphological level by a roughness of the fiber surface [Fig. 2(b)]. There appeared to be no relevant difference between the STEX whole straw and the STEX internode fraction.

Table I shows the changes in lignin and total reducing sugars content brought about by the STEX process, washing with water and extraction of lignin, first with ethanol then with acetone.

No activation was needed to dissolve the STEX wheat straw in DMAc–5% LiCl, but a certain amount of insoluble material (about 20%) was removed by centrifugation, washed with DMAc, and analyzed. This material was compared with the precipitate obtained by adding water to the DMAc–5% LiCl solution itself.

On comparing the results of the whole straw and the internode fraction, it can be seen that there is no substantial difference in composition. Furthermore, it can be seen that there is a loss of material (about 65–70%; Table I) during the different processes because of the chemical hydrolysis of the hemicelluloses and lignin,[3] a loss that can be mainly attributed to the STEX process. The starting values of the cellulose-to-hemicelluloses ratios, 1.4 for whole straw and 1.7 for its internode-enriched fraction, become about 10 for both materials after explosion and following treatment. In the final products, the hemicellulose content is 3–5%, while the percentage of cellulose increases from 40 to 80%, with better solubility characteristics.

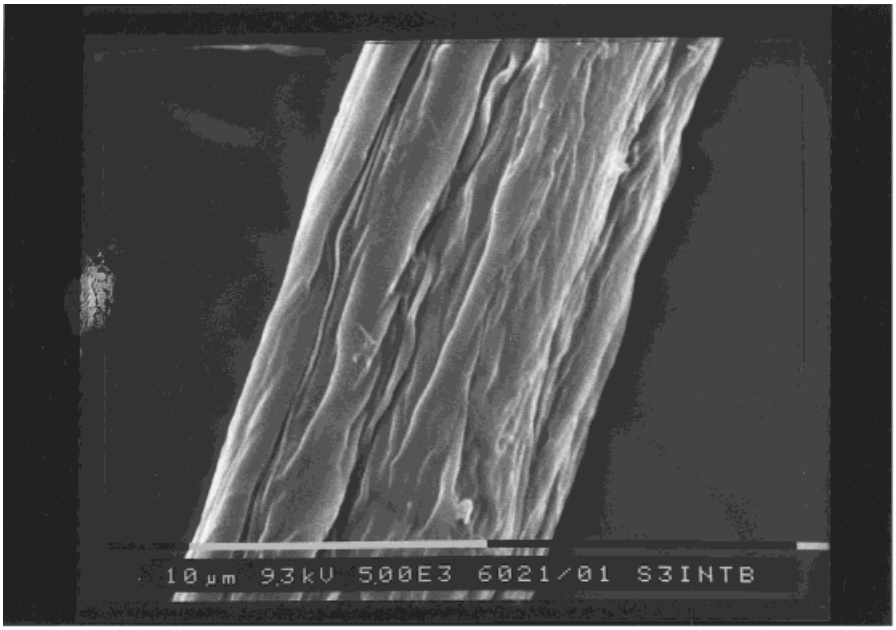

a)

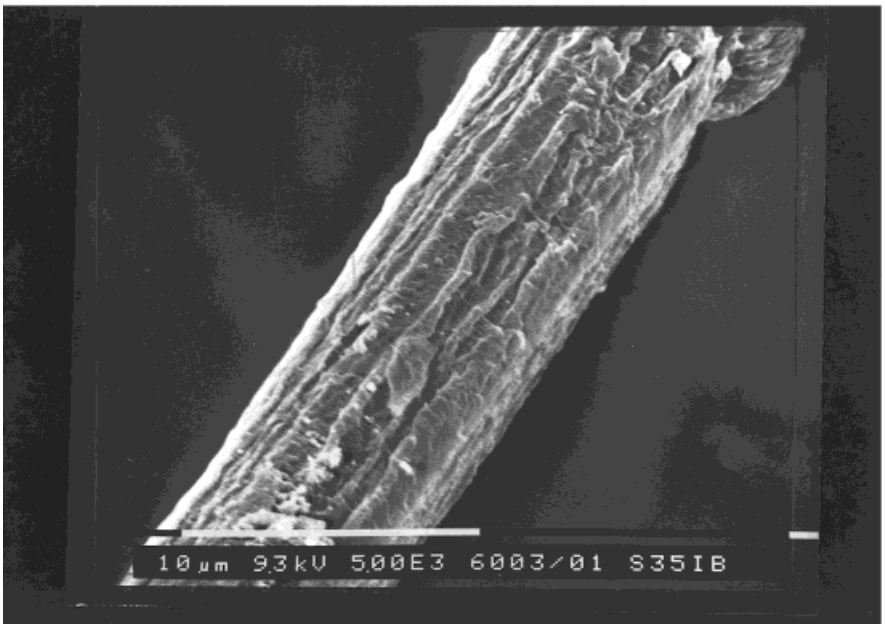

b)

Figure 2 SEM microphotographs of single fiber from (a) internode fraction and (b) STEX internode at 5000×.

Dilute solutions of bleached samples in DMAc–LiCI 5% were submitted to viscometric and light scattering measurements in accordance with the literature.[15] Molecularly dispersed entities were found to be present in the whole straw sample, while aggregate polymer species occur in the solution of the internode sample.

The preparation of cellulose tricarbanilates (CTC) was carried out by treating the DMAc–LiCl 5% solutions with phenylisocianate and changing the reaction variables, e.g., temperature, time, and amount of catalyst. Quantitative yields and complete substitution were obtained in milder reaction conditions than those conventionally used.[16] Table II shows the characteristics of CTC from whole straw and the internode fraction after STEX and bleaching. The viscometric and light scattering measurements were performed in THF. Integral

Table I Compositional Analysis

Samples	Klason Lignin (%)	Total Reducing Sugars (%)
Whole straw		
Untreated[a]	26	64
STEX straw	29	71
STEX extracted (H_2O) straw	33	67
STEX extracted (EtOH–acetone) straw	23	77
STEX straw prc[b]	14	86
STEX straw ins[c]	66	34
Internode straw		
Untreated[a]	26	64
STEX straw	31	69
STEX extracted (H_2O) straw	30	70
STEX extracted (EtOH–acetone) straw	23	77
STEX straw prc[a]	16	84
STEX straw ins[b]	49	51

[a] The 10% difference consisted of ash, protein, and volatile products.
[b] Precipitated from DMAc–LiCl solutions.
[c] Insoluble in DMAc–LiCl solutions.

distribution curves of the CTC, evaluated by HP/GPC (Fig. 3), indicate a polydispersity M_w/M_n matching that of commercial viscose.[17]

The composition of the unbleached materials (Table I) and the results concerning the bleached products (Table II; Fig. 3) suggest that after the steam explosion process, there are no relevant differences between whole straw and its internode fraction.

Characterization of Regenerated Fibers from STEX Straw

Whole straw and the internode fraction were subjected to the STEX process. Solutions in DMAc–LiCl 7% at different polymer content (Cp) were prepared without activation treatment at high temperatures, in the same way as for exploded wood.[17] The fact that there is no need for high temperature activation could, in practice, be relevant to the scaling up of the process to the industrial level. In the dissolution step, the samples behaved similarly, and the Cp obtained was up to 10%.

Fibers regenerated from the sample of the internode fraction using the wet spinning line were tested for their physicomechanical properties; it was observed that a general improvement in fiber

Table II Characteristics of CTC from Bleached STEX Straw

Sample	$N\%$[a]	ζ_{235} (mm)	$[\eta]$ (dL/g)
Bleached whole straw CTC $(DP_w)\zeta_s = 1079$	8.1	46.000	3.05
Bleached internodes CTC $(DP_w)\zeta_s = 810$	7.9	44.000	2.70

[a] Theoretical $N\%$ for DS 3 is 8.09.

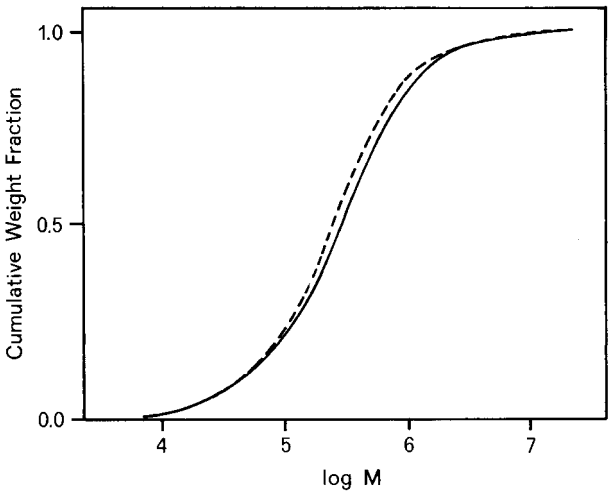

Figure 3 Integral distribution curves of CTC samples from (——) bleached STEX whole straw and (· · · · ·) bleached STEX internodes. M_w/M_n values are 6.5 and 5.5, respectively.

Table III Physicomechanical Properties of Regenerated Fibers Obtained from STEX Straw in DMAc–7% LiCl Solutions Spun at Variable Take-Up Speeds Using the Wet Spinning Line

STEX Samples	*Cp* (% w/w)	V_1/V_f	*DR*	*E* (Gpa)	σ (Gpa)	ε (%)
Bleached Whole Straw	4.0	1	0.39	13.0	0.24	6.6
	4.0	2	0.78	19.0	0.24	8.1
	6.9	1	0.39	13.8	0.30	nd[a]
	6.9	2	0.78	18.5	0.33	6.0
Bleached internodes	6.6	1	0.25	10.3	0.16	7.0
	6.6	2	0.49	12.0	0.20	6.8
	6.6	3	0.75	13.5	0.20	4.7
	7.9	1	0.43	12.2	0.20	6.3
	7.9	2	0.70	16.5	0.24	6.1
	7.9	3	1.05	17.5	0.23	5.0
	7.9	4	1.42	23.4	0.31	3.8
Unbleached internodes	5.3	1	0.25	12.2	0.25	8.3
	5.3	2	0.39	13.5	0.23	4.2
	5.3	3	0.76	17.0	0.30	4.1
	5.3	4	1.01	19.6	0.31	3.5

[a] nd = No data available.

properties was brought about by increasing the V_1/V_f draw ratio. Draw ratio values lower than 1 do not mean that fibers undergo a contraction in the coagulation bath. This effect is due to the die swelling, the relaxation of the filament at the die exit.[18,19] It is possible to value the true stretching of fibers by the V_1/V_f ratio. When this ratio was increased to values as high as 3–4, the fibers had good mechanical properties, with the modulus attaining 23.4 Gpa. These effects are evident both for bleached fibers and unbleached fibers containing high amounts of lignin.

The effect of lignin content on the behavior of the STEX samples during dissolution and spinning was assessed through conventional bleaching treatments. Unexpectedly, after bleaching, an activation step became necessary to reach high polymer concentrations, probably due to a higher aggregation of the cellulosic chains after hemicellulose elimination.

It was also found that using the wet spinning line under different spinning conditions resulted in fibers with interesting mechanical properties, comparable to those of rayon fibers from conventional processes and better than those obtained from STEX wood pulps (Table III). Furthermore, there appeared to be no significant differences in the mechanical properties of the regenerated fibers from the unbleached–bleached internode fraction and whole straw, providing suitable spinning parameters had been taken into account for the type of starting material.

The structural features of the regenerated fibers showing the best strength properties were investigated by different techniques to reveal any relationship between structural characteristics, physico-mechanical parameters, and processing parameters.

Cellulose polymorphic forms have been studied by X-ray diffraction (XRD) and, more recently, by CP-MAS ^{13}C-NMR and FTIR spectroscopy.[20] The X-ray diffractograms [Fig. 4(A)–(D)] of regenerated fibers exhibit a rather unresolved pattern that is most likely due to, in addition to the amorphous form, the merging of more polymorphic forms. The diffractograms of the regenerated fibers from whole straw and the internode fraction are not distinguishable; in both cases, there is intense diffraction (2θ) at 20.5° and a shoulder at 12.1°; according to Isogai et al., this would suggest the occurrence of the III_{II} crystalline form.[21] However, the rather low degree of crystallinity (65 $\pm$ 5%), as well as the presence of the cellulose II form evidenced by the deconvolution of the more intense X-ray reflection, could be responsible for the lack of purity of the crystalline forms in the samples. Increasing the take-up rate in the spinning led to no significant changes in the diffractogram pattern.

The CP-MAS ^{13}C-NMR spectra (Fig. 5) of the

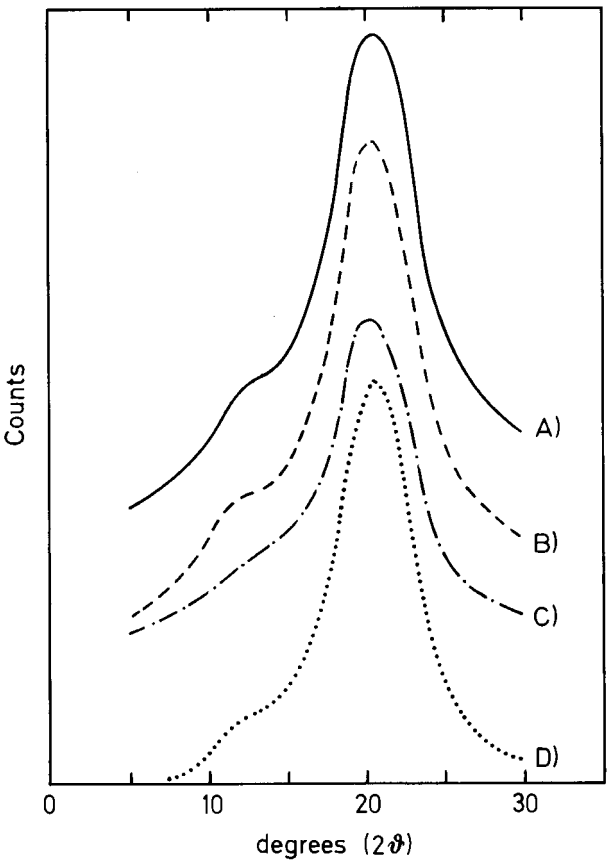

Figure 4 X-ray diffractograms of regenerated fibers: from bleached STEX whole straw (A) spun at $V_1/V_f = 1$; from bleached internode fraction: (B) spun at $V_1/V_f = 1$; (C) spun at $V_1/V_f = 2$; and (D) spun at $V_1/V_f = 3$.

regenerated fibers, independently of the sample origin, show very similar patterns. Such similarity has already been reported by one of us[22] for the cellulose III_{II} model and was since found in regenerated wood fibers.[17] A single resonance for C-1 appears at 104 ppm as well as for the signal arising from C-2, C-3, and C-5 carbon atoms at 75 ppm. Single broad signals for C-4 and C-6 carbons are shown at 83 and 63 ppm, respectively. The observed chemical shifts, in addition to the X-ray patterns, are quite close to the signals that Isogai et al. found in amorphous cellulose,[21] suggesting the superposition of more structural forms in the same sample. However, the intensity of the NMR peaks indicates a substantial order in the fibers; thus, as the X-ray crystallinity index of the regenerated straw fibers is rather low, it must be that there is an adequate orientation of the cellulose chains to account for the good mechanical properties. Actually, in all the examined samples, the orientation index of the disordered regions along the fiber axis was rather low (40–45%), but that of the crystalline regions quite high (75–80%).

The presence of anisotropy along the fiber was confirmed by Raman spectroscopy (Fig. 6–8). The Raman spectra of cellulose are already known,[23,24] and Atalla[25] has made further in-depth studies using polarized Raman in an effort to understand the assignment of the spectra bands and thus gain a greater understanding into molecular conformation and hydrogen bonding of cellulose polymorphs.

Figure 6 shows typical unpolarized spectra of straw regenerated fibers in the 3150–3500 cm^{-1} region of OH stretching. Fibers from both whole straw and the internode fraction or regenerated fibers in various spinning conditions (samples C and D) show several low intensity bands at different frequencies, suggesting nonuniform hydrogen bonding patterns in the samples.

The deconvoluted and second derivate Raman spectra (Fig. 7) in the region of the CH and CH_2 vibrations show an intense band at 2895 cm^{-1}, most likely due to methine CH bonds; while the 2985 and 2842 cm^{-1} bands are, respectively, plausible frequencies for antisymmetric and symmet-

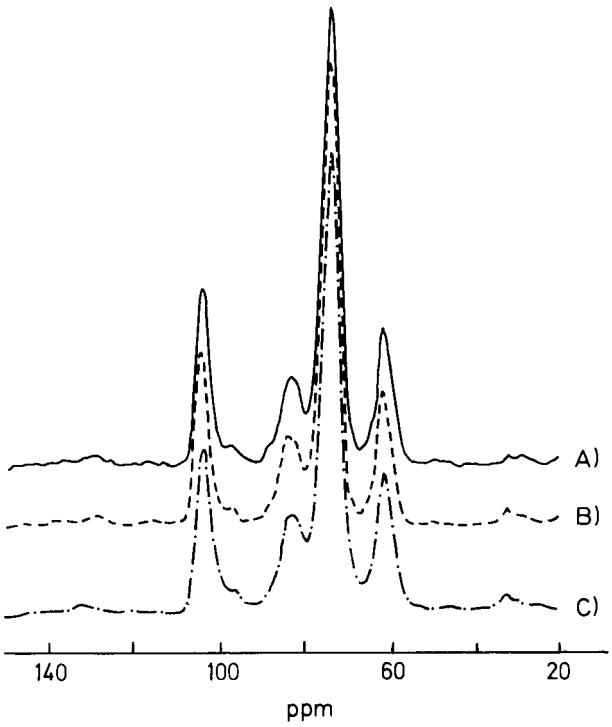

Figure 5 CP-MAS ^{13}C-NMR spectra of regenerated fibers from STEX straw (same samples (A)–(C) as in Fig. 4).

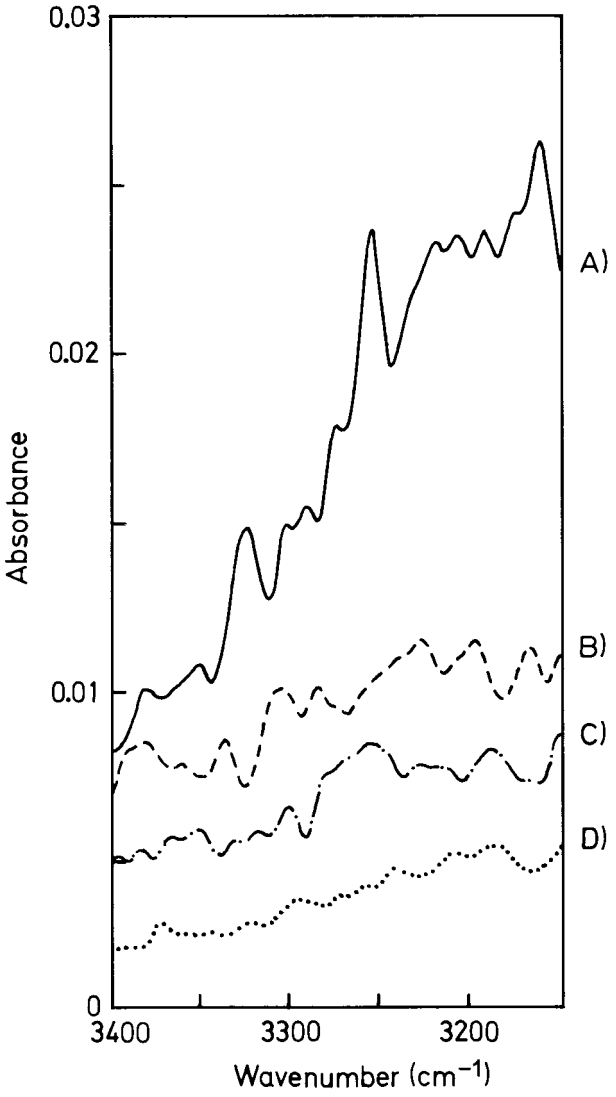

Figure 6 FT-Raman spectra of regenerated fibers from STEX straw in the 3500–3100 cm^{-1} region (same samples (A)–(D) as in Fig. 4).

ric CH_2 stretching vibrations. Nonspecific CH and CH_2 stretching vibrations occur in the spectrum of the regenerated straw fibers at 2811, 2932, and 2957 cm^{-1}, respectively, suggesting marked changes in the chain conformation with respect to fibrous native straw cellulose.

In the Raman spectra of the regenerated straw fibers, widely spaced bands can be seen associated to HCH, COH, and HCC bending vibrations in the 1000–1500 cm^{-1} region, a region particularly sensitive to polymorphic changes. Below 1000 cm^{-1}, numerous bands assigned to CC and CO stretching dominate; in the various regenerated straw samples, the band at 895 cm^{-1} (attributed at C-1-H bending mode) shows a different profile as well as a different width and intensity. This result could be related to both the degree of disorder and the crystallite sizes in the regenerated fibers.

The polarization of the Raman radiation provides information about the preferential orientation of the cellulose macromolecules. Figure 8 shows the Raman spectra recorded in the 800–1500 cm^{-1} region with the electric vector of the incident light parallel and perpendicular to the chain axis. The intensity of the 1098 and 1117 cm^{-1} skeletal bands is significantly higher in the parallel mode than in the perpendicular, indicating a preferential orientation of the anhydroglucose units in the direction of the cellulose chains. All the samples of regenerated fibers show anisotropy in the organization of the cellulose macromolecules.

REGENERATED FIBERS FROM STEX STRAW GRAFT COPOLYMERS

The use of lignocellulosic materials could be greatly expanded by modifying their properties for specific end use applications, and graft copolymerization is an excellent way to achieve this goal. For example, flexibility is sometimes required in packaging materials, in addition to high hydrophobicity and resistence to microbial attack. Such characteristics can be achieved through the grafting of a cellulose backbone with thermoplastic branches; this results in a decrease in the Young modulus and an increased breaking point of the material. Furthermore, the presence of lignocellulose graft copolymers can increase the compatibility of polymers of a different nature, such as cellulose and synthetic thermoplastic polymers.

As can be seen from Table IV, increasing the amount of monomer in the grafting reaction results in significant changes to the percentage add on, improving homopolymer and grafting efficiency; in fact, high add on and homopolymer yield was achieved by doubling the initial amount of monomer. On the other hand, the presence of a large amount of homopolymer that hinders macromolecule orientation can be a drawback in the dissolution and spinning processes. Without the elimination of the homopolymer, only highly concentrated (>15%) DMAc–LiCl solutions of STEX straw graft copolymers are spinnable.

Results on PAN-ground wheat straw graft copolymers have already been published.[26] The per-

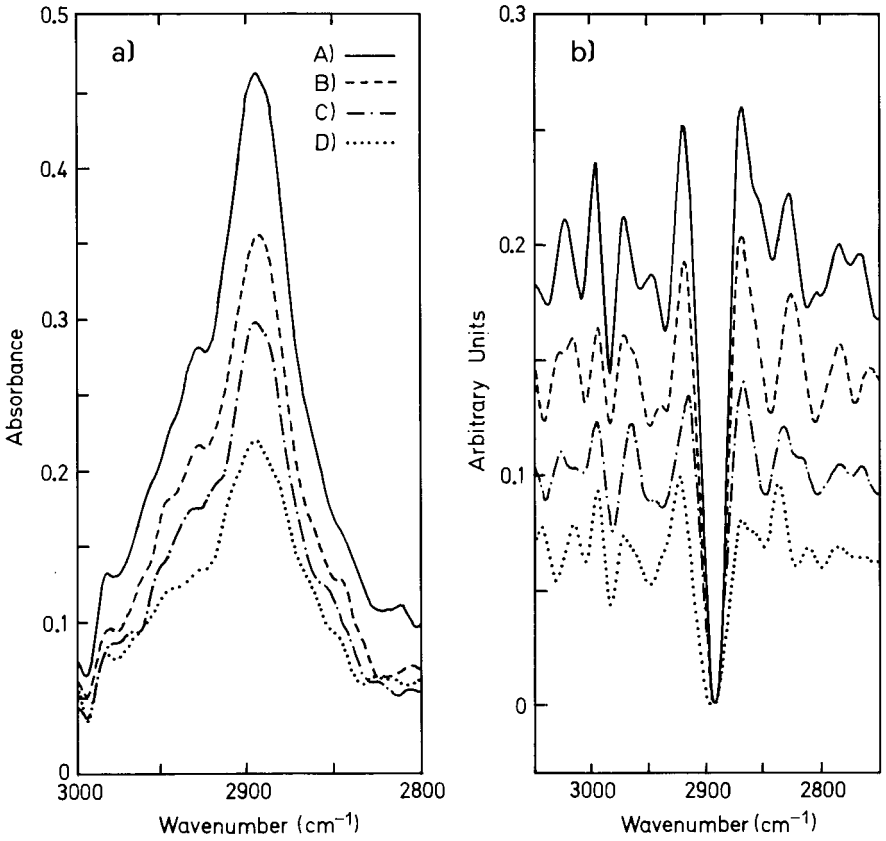

Figure 7 FT-Raman spectra of regenerated fibers from STEX straw in the 3100–2700 cm^{-1} region: (a) deconvoluted spectra; (b) second derivative spectra (same samples (A)–(D) as in Fig. 4).

centages of PAN-grafted polymer obtained using STEX straw was the same as for ground wheat straw, but less monomer and catalyst were needed and reaction times were shorter; similar results are found on comparing PMMA grafted onto both STEX straw and dissolving or groundwood pulps.[27] The molecular weight of the grafted chains obtained by intrinsic viscosity measurements after complete hydrolysis of the cellulose backbone was in the range of 5000–6000 daltons.

In order to have sufficient amounts of STEX-grafted straw for dissolution and spinning processes, further characterization, and an evaluation of the graft polymer properties, the reactions were carried out in a pilot plant using the best conditions for each graft copolymer (Table IV). The graft copolymers were dissolved in a DMAc–LiCl solvent system and spun on the dry jet laboratory-scale spinning line.

Any changes in the surface morphology of the fiber, due to the graft copolymers, were evident under the electron microscope. It was found that the surface features of the regenerated fibers from STEX straw-graft copolymers differed only slightly from those of ungrafted straw, with the striation being less evident. On examining the inner fracture surface of the fibers, the differences became more evident (Fig. 9), particularly in the fiber from STEX straw-grafted PAN copolymer where the lobed section appeared spongy (Fig. 10). Table V shows the mechanical properties of the regenerated fibers from the STEX straw graft copolymers.

Compared to the ungrafted STEX straw regenerated fibers, those from grafts on the cellulose chain have weaker strength properties due to the hindrance of macromolecule orientation during spinning, a result of the introduced copolymer side chains. This effect is particularly evident at a higher draw ratio. The strength parameters of both grafted fibers (from STEX wheat straw and internode) were found to be close to those of unbleached internodes still containing 25–27% lignin, with lignin possibly playing a negative role,

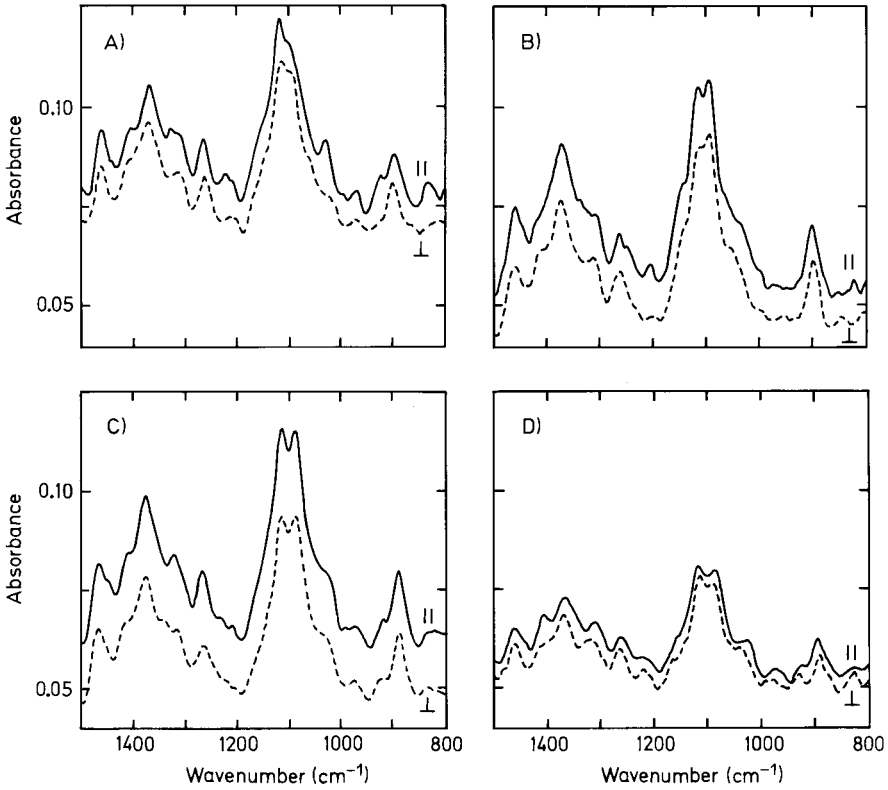

Figure 8 FT-Raman polarized spectra of regenerated fibers from STEX straw: (——) electric vector parallel; (· · · · ·) electric vector perpendicular (same samples (A)–(D) as in Fig. 4).

like that of grafting, on cellulose orientation during spinning.[28]

In the STEX straw, PAN, and PMMA copolymers, FTIR spectroscopy measurements of the grafted fibers showed the presence of the characteristic stretching vibration of CN at 2241 cm^{-1} and ester grafts at 1732 cm^{-1}, respectively. No chemical modification of the grafted polymers due to the dissolution process was observed.

The spinnability of the graft copolymers opens the possibility of using them in blends with cellulosic and synthetic fibers to prepare different end products, e.g., nonwovens and yarns, and to modify the properties of such products.

To verify how the grafted fibers can act as a compatibilizer between the parent cellulose and synthetic polymers, a differential scanning calorimetry (DSC) investigation was carried out on

Table IV Grafting of PAN and PMMA on STEX Straw Internode

Polymer	Monomer (mL)	Grafting[a] (%)	Homopolymer (%)	Efficiency of Grafting[b] (%)
PAN	0.87	44.1	11.2	75
PAN	1.75	57.5	23.2	60
PMMA	1.00	47.9	24.4	49
PMMA	2.00	65.9	42.9	35

[a] $\text{Grafting (\%)} = \dfrac{\text{(Final straw weight} - \text{Initial straw weight)}}{\text{Initial straw weight}} \cdot 100$

[b] $\text{Grafting efficiency (\%)} = \dfrac{\text{(Final straw weight} - \text{Initial straw weight)}}{\text{Total polymer weight after reaction} - \text{Initial straw weight}} \cdot 100$

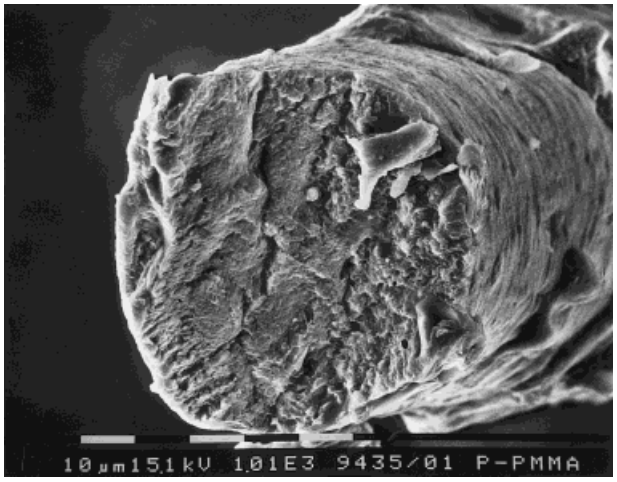

Figure 9 SEM photograph of fracture surface of STEX-straw-grafted PMMA fibers.

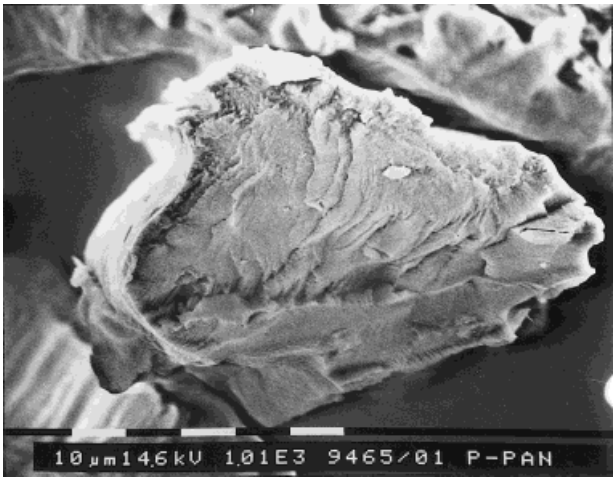

Figure 10 SEM photograph of fracture surface of STEX-straw-grafted PAN fibers.

the thermal behavior of blends of synthetic polymers and their STEX straw cellulose grafts. In the case of STEX-straw-grafted PMMA–PMMA blends (50 : 25 : 25), there was a marked decrease in the PMMA T_g value in the STEX straw–graft PMMA (from 121.7 to 67.5), a decrease that was even more enhanced in the straw-grafted PMMA–PMMA system (57.0). This indicates an increase in compatibility between natural and synthetic matrices in the presence of grafted components. In the case of grafted PAN copolymers, the effect of the grafted component on compatibility is less evident, with there being a 10% decrease in the PAN T_g value in the blends (STEX straw-grafted PAN–PAN in the ratio of 56: 33 : 11).

CONCLUSIONS

Steam explosion treatment has proved to be highly effective in inducing deep modifications of the molecular and supramolecular structure of wheat straw. Such structural modifications have made wheat straw a suitable raw material for dissolving and spinning processes, without any form of previous purification.

With the optimization of the spinning conditions as a function of the pulp composition and the spinning system (wet or dry jet), the feasibility to obtain regenerated fibers with commercially sound properties was proven. This opens good perspectives of scaling up a modulable process starting from different STEX straw pulps instead of

Table V Physicomechanical Properties of Grafted STEX Straw Regenerated Fibers in DMAc–7% LiCl Solutions Comparated with the Ungrafted Ones (Dry Spinning Line)

STEX Samples	*Cp* (% w/w)	V_0	*DR*	*E* (Gpa)	σ (Gpa)	ε (%)
g-PAN	7	42	1.02	8.4	0.11	4.4
g-PAN	7	42	1.26	8.2	0.11	2.5
g-PAN	7	42	1.52	6.8	0.10	3.1
g-PMMA internodes	7	42	1.02	9.0	0.12	3.9
g-PMMA internodes	7	42	1.26	9.4	0.13	4.1
g-PMMA internodes	7	42	1.52	7.8	0.10	4.5
Unbleached internodes	7	42	1.02	9.5	0.13	3.7
Internodes water washed	7	42	1.02	10.0	0.15	9.1
Internodes NAOH washed	7	28	0.96	14.7	0.21	6.0

highly purified pulps used in the conventional viscose process.

Furthermore, STEX wheat straw pulps can be used effectively as the starting material for the preparation of graft copolymers. As the properties of these products can be tailored to specific end use applications, further developments in the field could, in the short to medium term, greatly expand the utilization of wheat straw as a raw material for industrial use.

This work was partly supported by European Commission (DGXII) in the framework of Eclaire Project.

REFERENCES

1. E. A. Delong, *Can. Pat.* 1,096,374 (1980).
2. R. H. Marchessault, S. Coulombe, H. Morikawe, and D. Robert, *Can. J. Chem.,* **60,** 237 (1981).
3. M. Tanhasai, *Wood Res.,* **77,** 49 (1990).
4. B. Focher, A. M. Marzetti, and V. Crescenzi, *Steam Explosion Techniques: Fundamentals and Applications,* Gordon and Breach, Philadelphia, 1988.
5. P. B. Petersen, Separation and characterization of botanical components of straw in: Straw, a valuable raw material. *Proceedings of the International Symposium,* Piza Interu. Ltd Publ. Cambridge, U.K., 1987.
6. H. C. Hagedorn, *Biochem. Z.,* **46,** 1351 (1932).
7. M. Terbojevich, A. Cosani, M. Camilot, and B. Focher, *J. Appl. Polym. Sci.,* **55,** 1663 (1992).
8. M. L. Huggins, *J. Am. Chem. Soc.,* **64,** 2716 (1942).
9. B. Millaud and C. Strazielle, *Makromol. Chem.,* **180,** 441 (1979).
10. M. Terbojevich, A. Cosani, B. Focher, A. Naggi, and G. Torri, *Carbohydr. Polym.,* **18,** 35 (1992).
11. B. Valente, G. C. Alfonso, A. Ciferri, P. Giordani, and G. Marucci, *J. Appl. Polym. Sci.,* **26,** 3643 (1981).
12. Bruker Analitische Messtechnik GmbH, personal communication.
13. L. Segal, J. J. Creely, A. E. Martin, and C. H. Conrad, *Text. Res. J.,* **29,** 786 (1959).
14. G. Centola, G. Prati, and F. Riva, *Ric. Doc. Tess.,* **4,** 49 (1967).
15. M. Terbojevich, A. Cosani, G. Conio, A. Ciferri, and E. Bianchi, *Macromolecules,* **18,** 640 (1985).
16. R. Evans, R. H. Werane, and A. F. A. Wallis, *J. Appl. Polym. Sci.,* **37,** 3291 (1989).
17. B. Focher, A. Marzetti, G. Conio, E. Marsano, A. Cosani, and M. Terbojevich, *J. Appl. Polym. Sci.,* **51,** 583 (1994).
18. G. Conio, R. Bruzzone, A. Ciferri, E. Bianchi, and A. Tealdi, *Polym. J.,* **19,** 757 (1987).
19. E. Bianchi, A. Ciferri, G. Conio, and A. Tealdi, *J. Polym. Sci., Polym. Phys.,* **27,** 1477 (1989).
20. *The Structures of Celluloses, ACS Symposium Series 340,* R. H. Atalls Ed. American Chemical Society, Washington, DC, 1987.
21. A. Isogai, M. Usuda, T. Kato, T. Uryn, and R. H. Atalla, *Macromolecules,* **22,** 3168 (1989).
22. P. Sozzani, G. Torri, and B. Focher, in *From Molecular Materials to Solids,* F. Morazzoni, Ed., Polo Editoriale Chimico, Milano, Italy, 1993, Chap. 5.
23. J. Blackwell, P. D. Vasko, and J. L. Koenig, *J. Appl. Phys.,* **41,** 4375 (1970).
24. J. J. Cael, K. H. Gardner, J. L. Koenig, and J. Blackwell, *J. Chem. Phys.,* **62,** 1145 (1975).
25. R. H. Atalla, *Appl. Polym. Symp.,* **28,** 659 (1976).
26. G. F. Fanta, R. C. Burr, and W. M. Doane, *J. Appl. Polym. Sci.,* **33,** 899 (1987).
27. N. Nishioka, M. Yamaoka, H. Haneda, K. Kawakami, and M. Uno, *Macromolecules,* **26,** 4694 (1994).
28. H. Chanzy, M. Paillet, and R. Hagege, *Polymer,* **31,** 400 (1990).